Significant Band-Edge Light Emission from InGaAs RTDs: Evidence for the Universal Nature of Resonant- and Zener- Co-Tunneling

E. R. Brown,[1] W-D. Zhang,[1] T. A. Growden,[2] P. R. Berger,[2] R. Droopad[3]

[1]Dept. of Physics, Wright State Univ., Dayton, OH 45435, USA
[2]Dept. of Electrical and Computer Engineering, Ohio State Univ., Columbus, OH 43210, USA
[3]Ingram School of Engineering, Texas State Univ., San Marcos, TX 78666, USA

Abstract

We report strong light emission from a room-temperature n-type unipolar $In_{0.53}Ga_{0.47}As$/AlAs double-barrier resonant-tunneling diode (DBRTD) precisely at the $In_{0.53}Ga_{0.47}As$ band-edge near 1650 nm. The emission characteristics are very similar to what we have observed recently in GaN/AlN DBRTDs, both of which suggest that the mechanism for emission is cross-gap electron-hole recombination via resonant- and Zener co-tunneling of electrons, the latter mechanism generating the required holes. Analysis shows that because of the relatively small bandgap, the Zener tunneling probability can be large in this $In_{0.53}Ga_{0.47}As$/AlAs DBRTD and is a mechanism that may have been overlooked in the longstanding literature.

In recent research on n-type unipolar GaN/AlN DBRTDs, bright near-UV electroluminescence [1] has been discovered in addition to a reproducible negative differential resistance (NDR) at room temperature [2-6]. Through spectral measurements, the UV emission was found to be centered at the GaN band-gap wavelength around 365 nm, and through recent noise measurements that the transport displayed normal shot noise except for a suppression effect associated with the resonant tunneling. These results combined with detailed quantum transport computation [1] suggested that the near-UV emission was by cross-gap radiative recombination between electrons accumulated on the emitter side of the device, and holes created in the same region generated by Zener tunneling, which is enabled in vertical GaN heterostructures because of the huge polarization fields at the heterointerfaces [1, 7-10]. In this letter, we report on the first observation of the same mechanism for emission in an $In_{0.53}Ga_{0.47}As$/AlAs double-barrier RTD (DBRTD) but at the $In_{0.53}Ga_{0.47}As$ band-gap wavelength around 1650 nm. This discovery strongly suggests that the resonant- and Zener- co-tunneling of electrons is a universal feature of unipolar DBRTDs and, remarkably, one that has not been reported in the vast literature of resonant-tunneling diodes over the past 40+ years.

The DBRTD device under test was grown by molecular beam epitaxy as an $In_{0.53}Ga_{0.47}As$/AlAs heterostructure on a semi-insulating InP substrate with a layer structure and doping profile as shown in Fig. 1(a). Its active region is comprised of two unintentionally doped (UID) AlAs barriers (thickness=2.4 nm) separated by an undoped $In_{0.53}Ga_{0.47}As$ quantum-well (width = 4.4 nm) layer, such that a quasibound level E_1 occurs in the quantum well at an energy of ≈0.40 eV above the conduction band edge under zero bias. This rather high binding energy compared to typical DBRTDs means that a large bias is required to reach the condition of negative differential resistance (NDR), especially under forward bias (positive on top contact), because of the 100-nm low-doped spacer layer on the top side that depletes and supports a large voltage drop and electric field. A local peak in current occurs at the start of the NDR region at 1.80 V, and a valley at the end of the NDR region at 2.65 V with a peak-to-valley current ratio (PVCR) of 9.2, as displayed in the experimental I-V curve of Fig. 1(b). This excellent PVCR is characteristic of InGaAs vs GaAs-based DBRTDs going back to their first demonstrations [11-12]. Another important device metric is the peak current density J_P which is 3.5×10^4 A/cm^2 in this 9×6 μm^2 active-area device, making it a good RTD for fast electrical switching [13] amongst other possible high-speed applications.

Based on previous characterization of GaN/AlN RTDs, we assembled the set-up shown in Fig. 2(a) consisting of a precision I-V probe station, a near-IR light-emission detector, and a near-IR fiber spectrometer. The detector was a large-area Ge photodiode operating between 800 and 1800 nm and having a peak responsivity of 0.85 A/W at a wavelength of 1550 nm. Its input was coupled to the DBRTD with a short light pipe, and its output was dc coupled to a solid-state electrometer having a current noise floor of ~1 pA. Shown in Fig. 1(b) (right vertical axis) is the photocurrent from the Ge diode as a function of RTD bias voltage (L-V curve). The photocurrent from the electrometer rises significantly above the noise floor at a bias voltage of ≈1.0 V, and increases monotonically with higher voltage through the NDR region up to the valley point. Then there is a precipitous drop at the valley voltage followed by a slow increase above that. That is, the change in photocurrent in the NDR region is anticorrelated to the change in electrical current. This behavior is similar to that observed for the near-UV photocurrent from one of the GaN/AlN DBRTDs [1], but for reasons that are not yet understood.

The fiber spectrometer is a room-temperature InGaAs-array-grating instrument[14] sensitive between 880 and 1750 nm and has a programmable spectral resolution, chosen for the present experiments to be 0.5 nm. Plotted in Fig. 2 (b) are the spectral emission curves plotted vs wavelength and parameterized by bias voltage at V_B = 1.7, 2.1, 2.5, and 3.0 V. The middle two bias points are in the NDR region, and the first and last points are just below and above it, respectively. All four curves show a peak emission λ around 1580 nm, and a long-wavelength cut-off behavior around 1670 nm. The curves in the NDR region (i. e. V_B=2.1, 2.5V) were taken at their maximums as they varied over time due to self-oscillation in the NDR region. Superimposed in Fig. 2(b) is the $In_{0.53}Ga_{0.47}As$ band-edge wavelength reference, λ = 1649 nm corresponding to band-gap energy of 0.752 eV at 300 K. The intersection of this reference line with all four spectral curves in their steeply rising edge suggests that the observed emission is occurring at or near the $In_{0.5}Ga_{0.47}As$ band edge. However, the strongest curves in the NDR region (i. e. V_B=2.1, 2.5V) are distinctly asymmetric with short-wavelength tails that extend to 1300 nm or less. And the weaker emission curve at bias outside the NDR region (i. e. V_B=1.7, 3.0 V) also display short-wavelength tails, but appear more symmetric. We then examined the light emission with a UV fiber spectrometer. No peak feature was observed in the wavelength range of 200-800 nm. This and the IR spectrum suggest little possibility of recombination between confined electrons and holes in their respective potential wells.

To understand the emission process better, Fig. 2(c) shows the brightest of the emission curves plotted against the standard spontaneous emission expression for semiconductor electroluminescence [15]:

$$S(\nu) \propto \nu^2 (h\nu - E_G)^{1/2} \exp[(E_G - h\nu)/k_B T)] \quad (1)$$

where E_G is the $In_{0.53}Ga_{0.47}As$ band gap at room temperature, only the frequency-dependent terms are shown, and no external cavity effects are included. The fit is reasonable on the low frequency (long-wavelength) end, but obviously is much faster decaying than the experiment on the short-wavelength end.

A simple qualitative model that explains the experimental data is shown schematically in Fig. 3(a). The emission spectra of Fig. 2(b), (c) clearly indicate that the emission is most likely free-carrier cross-gap recombination occurring at the $In_{0.53}Ga_{0.47}As$ band edge, which requires free holes. Judging from the threshold in emission shown in Fig. 1(b) just below 1.0 V bias, the likely generation mechanism for holes is the Zener tunneling mechanism of Fig. 3(a). The bias condition in 3 (a) is such that electrons can flow readily from the emitter to the collector through the quantum well quasibound level, but also empty conduction band states on the collector side are made available to valence band states at the same energy on the emitter side. Hence, Zener tunneling can occur while conserving energy and crystal momentum. The lowest possible threshold bias for this process is approximately the $In_{0.53}Ga_{0.47}As$ bandgap of ≈0.75 eV, which is reasonably close to the experimental threshold. Note that this model is subtly different than that proposed for the GaN/AlN DBRTD in Ref. 1 where it appeared the Zener tunneling likely happens on the collector side followed by transport of the holes to the emitter side where radiative recombination occurred. This is because in GaN the key factor in the Zener tunneling is the huge interfacial polarization field [7], whereas with $In_{0.53}Ga_{0.47}As$ the key factor is the narrow bandgap.

To confirm that Zener tunneling makes sense in the present structure, we present a calculation of the valence-to-conduction band tunneling probability according to the classic Kane expression:

$$T = \frac{\pi^2}{9} exp\left(-\frac{\pi^2 E_G^2 \cdot m}{2hP \cdot F}\right) \quad (2)$$

where m is the electron mass in vacuum, h is Planck's constant, P is the momentum matrix element between the valence and conduction band cell-periodic wavefunctions, generally expressed as $E_P \equiv P^2/2m$, and F is the electric field in units of eV/cm [16-17]. Strictly speaking this expression applies to interband tunneling through a band-gap barrier supporting a uniform electric field, but that happens to be a reasonable approximation in the present DBRTD because of the low-doped spacer layer on the collector side and the gradual band bending that occurs there, as shown qualitatively in Fig. 3 (a). So we plot in Fig. 3(b) the expression in (2) assuming $E_G = 0.752$ eV, $E_P = 25.3$ [18], and as a function of F between 1.0×10^5 and 3.0×10^5 eV/cm. The tunneling probability increases more than 6-orders-of-magnitude over this range of bias field, which is essentially a decaying exponential dependence on the length of the band-gap barrier given approximately as $L_B \approx E_G/F$. Between the bias voltage where we first see significant light emission, $V_B \approx 0.75$ eV, and the peak voltage $V_B = 1.80$ V, we observe T increase ~50 times from 2×10^{-7} to 1×10^{-5}. While these values may at first seem small compared to the transmission values for resonant tunneling, which routinely fall in the range 0.1 to 1.0, the overall Zener tunneling current also depends on the "supply function" of electrons occupying the valence band on the emitter side, which is very large because of the high effective density-of-states and the near-unity Fermi occupancy factor.

The qualitative model of Fig. 3(a) might also explain the much broader experimental emission peak than described by Eqn. (1). The holes created by Zener tunneling occupy a normal 3D valence band, but the electrons are subject to occupation of the quasi-2D region in the undoped spacer layer adjacent to the barriers on the emitter side. This so called "pre-well" has been the subject of debate over the years in the context of DBRTD design and speed limits. Here, it can have the effect of smearing out the recombination spectral signature. A hole such as that shown in Fig. 3(a) that is created at (or diffuses to) the peak of the band profile on the emitter side will emit photons very close to the band edge. However, a hole that is created in the "pre-well" region can only recombine with electrons that occupy the pre-well quasibound level or above [shown as E_C in Fig. 3(a)], which is significantly elevated above the conduction band edge. Therefore, the emitted photon will have energy significantly above E_G, consistent with the experimental data in Fig. 2(b), (c). Whether or not this simple model can explain the anti-correlation in the NDR region between the electrical current and photocurrent shown in Fig. 2(b) remains to be seen, as this is a more complicated effect involving coupled quasibound states.

The emitted absolute power and the internal quantum efficiency were estimated from the photocurrent in Fig. 2(a) and the Ge photodiode responsivity, indicating the emitted power is at the few nW level. However, the DBRTD under test is not designed for efficient light emission but rather for high-speed electrical performance, meaning that the active device is a vertical mesa with small active area and a top ohmic contact that is opaque to all radiation wavelengths of interest. So the radiation can only escape the mesa through the sidewalls, propagating out in a cylindrical ring, and the light-pipe coupled to the Ge photodiode collects only a small fraction of this (~1%). Altogether, these effects lead to a rough estimation of 0.1% for the external quantum efficiency (EQE). Better design of the DBRTD as a light emitter using a transparent top contact or faceted sidewalls, for example, should improve the EQE dramatically.

In conclusion, unipolar-doped double-barrier RTDs have now been shown to manifest electron resonant and Zener (interband) co-tunneling in two different materials systems, the historic $In_{0.53}Ga_{0.47}As$/AlAs system described here for the first time. This mechanism creates holes at the emitter side of the structure where electrons are heavily accumulated, leading to band-to-band light emission. This has been an overlooked feature of RTDs since their invention in 1973 [19].

This work was supported by the U.S. National Science Foundation (under Grant #1711733), Program Director Dr. Dimitris Pavlidis.

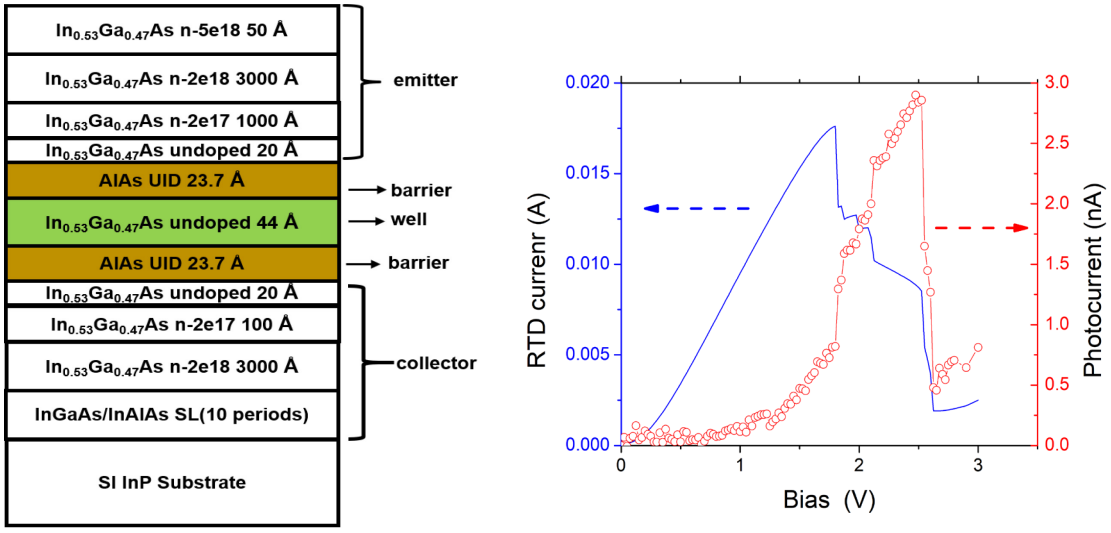

(a) (b)

Fig. 1. (a) Epitaxial layer structure for InGaAs/AlAs RTD. (b) Room-temperature I-V curve (left vertical axis), and L-V curve measured with the NIR Ge photodiode shown in Fig. 2(a).

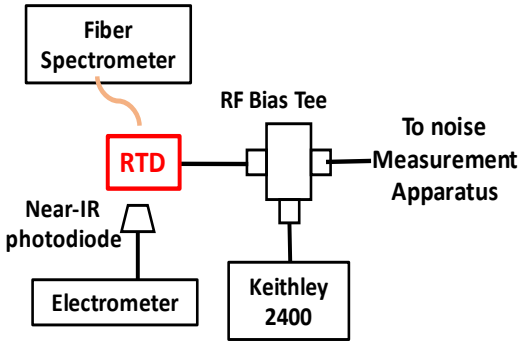

(a)

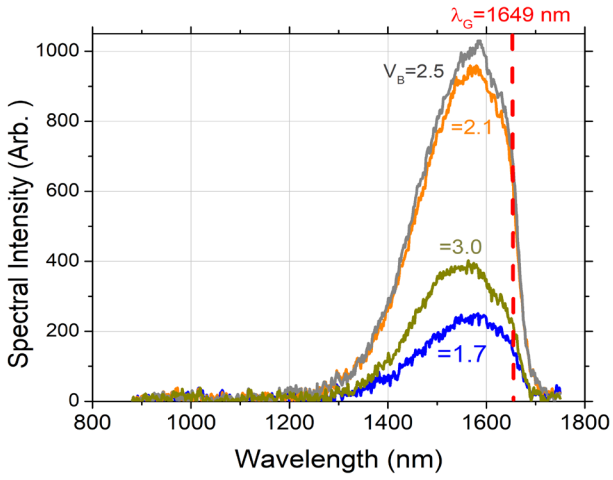

(b)

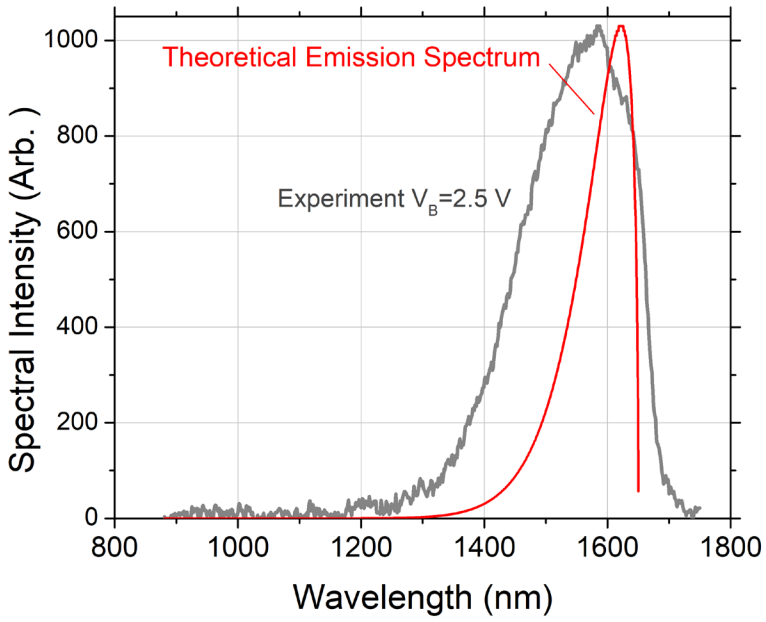

(c)

Fig. 2. (a) Experimental set-up used to measure I-V curves, total light emission, and spectrally resolved emission. (b) Spectrally resolved emission at four different bias voltages. (c) Spectral emission at the most intense spectrum in (b) and the plot of theoretical electro-luminescence according to Eqn. 1.

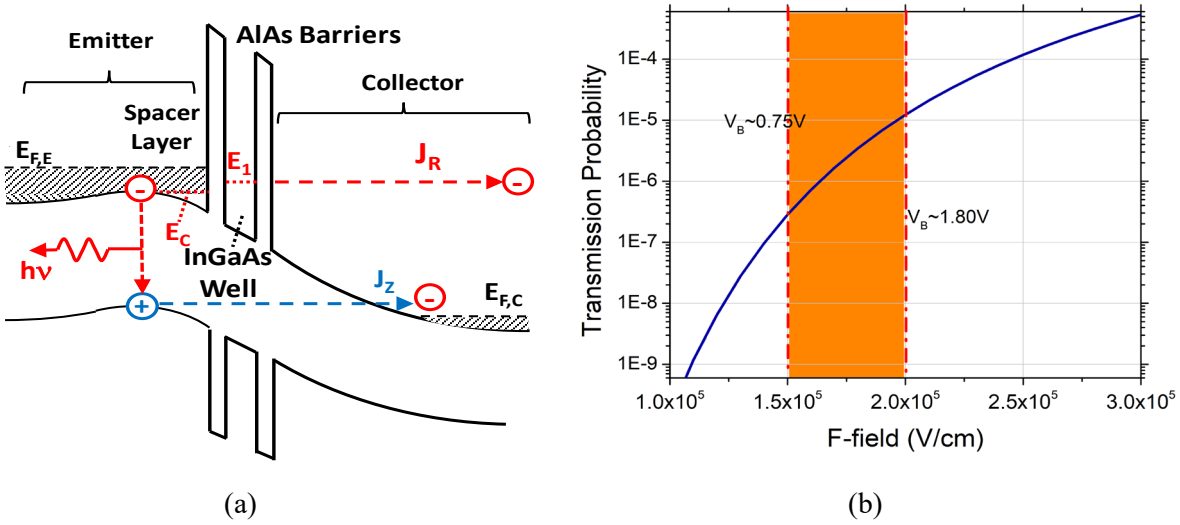

(a) (b)

Fig. 3. (a) Band bending model with positive bias below the NDR region showing simultaneous electron resonant- and Zener-tunneling. (b) Zener tunneling probability according to Kane model over the range of bias fields in the present device, along with bias voltages at the boundary fields.

References

1. Growden, T. A., Zhang, W. D., Brown, E. R., Storm, D. F., Meyer, D. J, and Berger, P. R. Near-UV Electroluminescence in Unipolar-Doped, Bipolar-Tunneling (UDBT) GaN/AlN Heterostructures. *Nature Light: Science & Applications* **7**, 17150 (2018).
2. Kikuchi, A., Bannai, R., Kishino, K., Lee, C-M., Chyi, J-N. AlN/GaN double-barrier resonant tunneling diodes grown by rf-plasma-assisted molecular-beam epitaxy. *Appl. Phys. Lett.* **81**, 1729 (2002).
3. Bayram, C., Vashaei, Z., Razeghi, M. AlN/GaN double-barrier resonant tunneling diodes grown by metal-organic chemical vapor deposition. *Appl. Phys. Lett.* **96**, 042103 (2010).
4. Growden, T. A., Storm, D. F, Zhang, W-D., Brown, E. R., Meyer, D. J., Fakhimi, P., and P.R. Berger, P. R. Highly repeatable room temperature negative differential resistance in AlN/GaN resonant tunneling diodes grown by molecular beam epitaxy. *Appl. Phys. Lett.* **109**, 083504 (2016).
5. Encomendero, J., Faria, F. A., Islam, S. M., Protasenko, V., Rouvimov, S., Sensale-Rodriguez, B. , Fay, P. , Jena, D. , and Xing, H.G. New Tunneling Features in Polar III-Nitride Resonant Tunneling Diodes. *Phys. Rev. X 7*, 041017 (2017).
6. Growden, T. A., Zhang, W-D., Brown, E.R., Storm, D. F., Hansen, K., Fakhimi, P., Meyer, D. J., and Berger, P. R. 431 kA/cm^2 peak tunneling current density in GaN/AlN resonant tunneling diodes. *Appl. Phys. Lett.* **112**, 033508 (2018).
7. Ambacher, O., Foutz, B., Smart, J., Shealy, J. R., Weimann, N. G., *et al*. Two-dimensional electron gases induced by spontaneous and piezoelectric polarization in undoped and doped AlGaN/GaN heterostructures. *J Appl Phys* 2000; **87**: 334-344.
8. Grundmann, M. J., Mishra, U. K. Multi-color light emitting diode using polarization-induced tunnel junctions. *Phys Status Solidi* 2007; **4**: 2830-2833.
9. Simon, J., Zhang, Z., Goodman, K., Xing, H., Kosel, T., Fay P., and Jena D. Polarization-Induced Zener tunnel junctions in wide-band-gap heterostructures. *Phys. Rev. Lett.* **103**, 026801 (2009).
10. Schubert, M. F. Interband tunnel junctions for wurtzite III-nitride semiconductors based on heterointerface polarization charges. *Phys Rev B* 2010; **81**: 035303.
11. Broekaert, T. P. E., Lee, W., and Fonstad, C. G. Pseudomorphic $In_{0.53}Ga_{0.47}As$/AlAs/InAs resonant tunneling diodes with peak-to-valley current ratios of 30 at room temperature. *Appl. Phys. Lett.* **53**, 1545 (1988).
12. Inata, T.,Muto, S., Nakata, Y., Sasa, S., Fujii, T., and Hiyamizu, S.APseudomorphic $In_{0.53}Ga_{0.47}As$/AlAs resonant tunneling barrier with a peak-to-valley current ratio of 14 at room temperature. Janpanese Journal of Applied Physics. 26, L1332-L1334 (1987).
13. Growden, T. A., Brown, E. R., Zhang, W-D., Droopad, R. , and Berger. P. R. Experimental determination of quantum-well lifetime effect on large-signal resonant-tunneling diode switching time. *Appl. Phys. Lett.* **107**, 153506 (2015).
14. Stellarnet, Inc. "DWARF-Star" NIR spectrometer; www.stellarnet.us
15. Sze, S. M. Physics of Semiconductor Devices, 2nd Ed., (John Wiley and Sons, New York, 1981).
16. Kane, E. O. Zener tunneling in semiconductors. *J. Phys. and Chem. of Solids* **12**, 181-188 (1959).
17. Vandenberghe, W., Soree, B., Magnus, W., and Groeseneken, G. Zener tunneling in semiconductors under nonuniform electric fields. *J. Appl. Phys.* **107**, 054520 (2010).
18. Vurgaftman, I., Meyer, J. R., and Ram-Mohan, L. R. . Band parameters for III-V compound semiconductors and their alloys. *J. Appl. Phys.* **89**, 5815 (2001).
19. Tsu, R. and Esaki, L.Tunneling in a Finite Superlattice. *Appl. Phys. Lett.* **22**, 562 (1973).